Disentangling drought-responsive traits with focus on Arabidopsis

Thonglim, A.

Chapter 4

High leaf water potential: a key to drought resilience in *JUB1* overexpression lines of Arabidopsis and tomato

*Ajaree Thonglim[1, *], Giovanni Bortolami[1], Sylvain Delzon[2], Maximilian Larter[2], Erik Smets[1,3], Salma Balazadeh[4], and Frederic Lens[1,3, *]*

Manuscript in preparation for publication

[1] Naturalis Biodiversity Center, Research Group Functional Traits, PO Box 9517, 2300 RA Leiden, The Netherlands

[2] BIOGECO INRA, Université Bordeaux, 33615 Pessac, France

[3] Leiden University, Institute of Biology Leiden, Plant Sciences, Sylviusweg 72, 2333 BE Leiden, The Netherlands

[4] Leiden University, Institute of Biology Leiden, Molecular Plant Stress Biology, Sylviusweg 72, 2333 BE Leiden, The Netherlands

* Correspondence: ajaree.thonglim@naturalis.nl and frederic.lens@naturalis.nl

Abstract

Increased drought events caused by climate change are leading to yield stagnation and crop losses worldwide, emphasizing the importance of understanding drought tolerance mechanisms for resilient crop development. JUNGBRUNNEN1 (JUB1), a multifunctional transcription factor, has been identified as a positive regulator of drought tolerance in various species. However, the mechanisms underlying *JUB1*'s enhancement of drought tolerance remain unexplored. To address this knowledge gap, our study comprehensively analyzed anatomical and hydraulic traits in well-watered and water deficit conditions, including intervessel pit membrane thickness (T_{PM}), stem lignification, embolism resistance in stems (P_{50}), stomatal safety margin (SSM), stomatal conductance (g_s), and leaf water potential (Ψ_l), in wild-types and *JUB1* overexpression (OX) lines of *Arabidopsis thaliana* and *Solanum lycopersicum* (tomato). Our results highlight the pivotal role of maintaining high Ψ_l in conferring drought tolerance in the more resilient *JUB1OX* genotypes, both in Arabidopsis and tomato. Interestingly, none of the stem anatomical features nor any of the hydraulic traits associated with drought tolerance in other Arabidopsis genotypes showed a correlation with the improved drought response of the *JUB1OX* genotypes. Even more surprisingly, *JUB1OX* plants exhibited traits typically associated with reduced resilience to drought, such as (slightly) less negative stem P_{50}, narrower SSMs, and thinner intervessel pit membranes. When looking more into stomatal conductance dynamics that may be involved in stabilizing Ψ_l during drought between *JUB1OX* genotypes and wild-types in Arabidopsis and tomato, we see that A-*JUB1OX* plants lose less water via transpiration through a lower initial g_s during well-watered conditions and early drought compared to the wild-type and *jub1* knockdown mutant, while the stomata in A-*JUB1OX* plants take longer to completely close. In tomato *JUB1OX* plants, however, we observed elevated g_s during the initial stages of drought compared to the wild-type tomato plants, followed by a steep decline until the stomata are fully closed. In conclusion, our findings highlight that high leaf water potential is central in the mechanism contributing to the enhanced drought tolerance observed in *JUB1OX* plants, but none of the other traits investigated shows evidence of how these plants stabilize their Ψ_l levels during conditions of water deficit. This opens the door to investigating in detail the role of *JUB1* on the accumulation of osmoprotectants such as proline in the leaves.

Keywords: *Arabidopsis thaliana*, *Solanum lycopersicum*, drought response, embolism resistance, leaf water potential, stem anatomy, stomatal conductance.

Introduction

Water availability is a crucial factor that has a significant impact on plant growth and productivity. As plants rely on water for their development and functioning, limited water availability is a significant constraint on plant growth (Choat *et al.*, 2018; Martinez-Vilalta *et al.*, 2019; Sapes *et al.*, 2019; Brodribb *et al.*, 2020). Ongoing climate change has led to rising temperatures and shifting rainfall patterns, increasing the frequency and severity of droughts that exacerbate water scarcity worldwide (Kim and Jehanzaib, 2020; Fischer *et al.*, 2021). Approximately 75% of the global harvested area is affected by lower water availability (IPCC, 2022), resulting in reduced photosynthesis, yield stagnation, and crop losses that have been increasing globally in recent decades (Matiu *et al.*, 2017; Sultan *et al.*, 2019; Agnolucci and De Lipsis, 2020; Brás *et al.*, 2021). Ultimately, drought could lead to plant mortality, which is a complex process that associates the interplay between water and carbon interdependencies (Anderegg *et al.*, 2015; McDowell *et al.*, 2022). Among the various mechanisms involved in drought-induced plant mortality, hydraulic failure is considered the primary cause and occurs when plants experience extreme water stress due to short intense droughts, leading to the collapse of the water transport system (Sperry and Tyree, 1988; Venturas *et al.*, 2017; McDowell *et al.*, 2022; Johnson *et al.*, 2022). Under conditions of soil drying and high evaporative demand, the tension in the xylem increases, triggering the formation of large gas bubbles in the water-conducting cells (embolisms), although the precise mechanisms of embolism formation in the xylem remain incompletely understood (Lens *et al*., 2022). There is increasing evidence, however, that embolisms spread via the interconduit pit membranes among adjacent conduits (air-seeding), causing a massive decline in hydraulic conductance that will provoke desiccation of plant tissues, cell death, and, ultimately, plant death (Brodribb and Cochard, 2009; Urli *et al.*, 2013; Adams *et al.*, 2017; Mantova *et al.*, 2022*a,b*; McDowell *et al.*, 2022).

Bearing this in mind, it is clear that determining the critical levels of embolism in plants' xylem is important for understanding their drought tolerance. The lethal level of embolism that is irrecoverable for plants is thought to be close to P_{88} (referring to xylem pressure leading to 88% loss of maximum conductance) (Hammond *et al.*, 2019; Johnson *et al.*, 2021; Mantova *et al.*, 2021, 2022*b*). While there are concerns that P_{88} may not be precise enough as an estimate of the point-of-no-return (Hammond *et al.*, 2019; Johnson *et al.*, 2021; Mantova *et al.*, 2021, 2022*b*), P_{50} or the pressure inducing 50% loss of hydraulic conductance is commonly used as a proxy for tolerance to xylem embolism (Tyree and Ewers, 1991; Maherali et al., 2004; Choat *et al.*, 2012; Venturas et al., 2017; Brodribb, 2017). The stomatal safety margin (SSM), referring to the difference between the water potential at stomatal closure (Ψ_{gs90}) and P_{50}, is often regarded as an even more reliable parameter to estimate drought resilience, because it takes also into account dynamics of stomatal regulation (see next paragraph; Meinzer *et al.*, 2009; Choat *et al.*, 2012; Anderegg *et al.*, 2016; Martin-StPaul *et al.*, 2017; Eller *et al.*, 2018; Creek *et al.*, 2020; Dayer *et al.*, 2020; Skelton *et al.*, 2021; Oliveira *et al.*, 2021).

Plants have evolved a range of strategies to cope with the detrimental effects of drought-induced embolism on their growth and survival, and to maximize their performance and fitness during water shortages (Violle *et al.*, 2007). These mechanisms operate at various scales, involving processes at the morphological, anatomical, physiological, and molecular levels, and include multiple drought-related traits in different organs that act in concert to maintain metabolic activity without risking plant mortality (Allen *et al.*, 2009; Lata and Prasad, 2011; Choat *et al.*, 2012; Mitchell *et al.*, 2013; Basu *et al.*, 2016; Brodribb *et al.*, 2017*b*; Thonglim *et al.*, 2023; Limousin *et al.*, 2022). Stomata closure is one of the initial responses to drought, occurring before embolism formation (Brodribb *et al.*, 2003; Martin-StPaul *et al.*, 2017; Scoffoni *et al.*, 2017; Choat *et al.*, 2018). This process can be triggered by the production of abscisic acid (ABA) or ethylene in leaves as well as leaf turgor changes, which signals the guard cells in the stomata to close, leading to a significant reduction in water loss via transpiration and thereby helping to maintain high leaf water potential (Ψ_l) (Desikan *et al.*, 2006; Tombesi *et al.*, 2015; Kuromori *et al.*, 2018). At the same time, stomatal closure also results in reduced CO_2 assimilation and photosynthetic activity (McDowell *et al.*, 2008; Brodribb *et al.*, 2017*b*;

Martínez-Vilalta and Garcia-Forner, 2017; Martin-StPaul *et al.*, 2017; Knipfer *et al.*, 2020). Plants also have the ability to modify their xylem anatomy to better avoid embolism formation and spread. For example, thicker intervessel pit membranes in angiosperms have been shown to better prevent the spread of embolisms between adjacent vessels (Lens *et al.*, 2011, 2022; Li *et al.*, 2016; Gao *et al.*, 2019; Kaack *et al.*, 2019, 2021; Zhang *et al.*, 2020; Thonglim *et al.*, 2021, 2023; Levionnois *et al.*, 2021; Isasa *et al.*, 2023). In addition, increasing stem lignification levels in otherwise non-woody lineages (Lens *et al.*, 2011, 2016; Dória *et al.*, 2018; Thonglim *et al.*, 2021, 2023) or modifying lignin composition enhances embolism resistance (Pereira *et al.*, 2018; Ménard *et al.*, 2022). Alternatively, plants can recover from massive embolism events by developing new wood tissue (Gauthey *et al.*, 2022), or they can prevent these detrimental embolism events by building more resistant xylem in combination with rapid stomatal closure leading to a large stomatal safety margin (SSM) (Creek *et al.*, 2020; Thonglim *et al.*, 2023). In addition to a wide range of physiological and anatomical adaptations, plants also respond to drought at the molecular level through the coordinated regulation of gene expression (Singh *et al.*, 2022). Under drought stress, water deficit triggers a reprogramming of the transcriptome, in which transcription factors (TFs), and gene regulatory networks (GRNs) play a critical role (Rabara *et al.*, 2014; Todaka *et al.*, 2015; Vermeirssen *et al.*, 2015; Chen *et al.*, 2016*b*; Joshi *et al.*, 2016). In the last decades, several NAC TFs in many different plant species have been identified as important regulators of responses to biotic and abiotic stresses, and have been shown to be useful for improving drought tolerance in crops (Le *et al.*, 2011; Al Abdallat *et al.*, 2014; Fang *et al.*, 2015; Sakuraba *et al.*, 2015; Wang *et al.*, 2016*b*).

JUNGBRUNNEN1 (JUB1) is a multifunctional TF of the NAC family in *Arabidopsis thaliana* that plays a central role in regulating plant longevity and the interplay between growth and stress responses (Shahnejat-Bushehri *et al.*, 2012, 2016; Wu *et al.*, 2012). JUB1 functions as a positive regulator of drought tolerance not only in Arabidopsis but also in other species such as tomato and banana (Tak *et al.*, 2017; Thirumalaikumar *et al.*, 2018). The overexpression of *JUB1* (*JUB1OX*) strongly delays senescence and enhances drought tolerance, while the *JUB1* knockdown (*jub1kd*) mutant exhibits a drought sensitivity (Shahnejat-Bushehri *et al.*, 2012; Wu *et al.*, 2012; Ebrahimian-Motlagh *et al.*, 2017; Thirumalaikumar *et al.*, 2018). Even

though the mechanistic role of *JUB1* on drought tolerance is unclear, there is evidence suggesting its effect on enhancing the osmoprotectants accumulation (Wu *et al.*, 2012; Shahnejat-Bushehri *et al.*, 2017; Tak *et al.*, 2017; Alshareef *et al.*, 2019; Welsch, 2022) as well as lowering reactive oxygen species (ROS) levels in leaves (Shahnejat-Bushehri *et al.*, 2012, 2016; Wu *et al.*, 2012; Ebrahimian-Motlagh *et al.*, 2017; Thirumalaikumar *et al.*, 2018). In addition, nothing is known about *JUB1OX's* impact on the underlying physiological response to drought and on the stem anatomical and hydraulic traits that are associated with embolism resistance.

In this study, we investigate the stem anatomical (proportion of stem lignification, intervessel pit membrane thickness) and hydraulic traits (stem P_{50}), and quantified the drought response in wild-type and *JUB1* overexpression (*JUB1OX*) transgenic lines of *Arabidopsis thaliana* and tomato (*Solanum lycopersicum* L.). During the drought treatment, gas exchange, and leaf water potential (Ψ_l) dynamics were measured and complemented with stem P_{50} to calculate the SSM. We aimed to assess whether or not *JUB1OX* in Arabidopsis and tomato uses a set of integrated leaf and stem traits to enhance drought resilience. More in particular, we addressed the following research questions: (i) Do the *JUB1OX* transgenic lines in Arabidopsis and tomato develop the expected anatomical (more lignified stem, thicker intervessel pit membranes) and ecophysiological traits (more negative P_{50}, larger SSM, lower g_s, higher Ψ_l) that are known to be associated with improved drought response in other taxa? (ii) Are there any consistent differences in the traits investigated between the wild-type and *JUB1OX* genotypes in both species?

Materials and methods

Plant material and growth conditions

The model plant, *Arabidopsis thaliana* (L.) Heynh. and the crop species *Solanum lycopersicum* L. (tomato) were investigated. For Arabidopsis, we studied the Columbia-0 (Col-0) ecotype (wild-type), and two transgenic lines in the Col-0 background: with one genotype with *JUNGBRUNNEN1* (*JUB1*) gene being overexpressed (*JUB1OX*), and another mutant line (*jub1kd*) where the expression of *JUB1* was knocked down. For tomato, we used one wild-type cultivar, *Solanum lycopersicum* L. cv. Moneymaker (MM), and one transgenic line *JUB1OX* in the MM background. To differentiate the same transgenic lines between both species, we added A- and T- prefixes to assign genotypes to either Arabidopsis or tomato.

Arabidopsis plants

The seeds of each genotype were germinated directly into a mixture of soil and sand (ratio 4.5:1). At 10-12 days after germination, the healthy seedlings were transferred to 8 cm-diameter pots and grown individually under controlled growth chamber conditions. The growth chamber was set to maintain a 20°C temperature during the day and a 17°C temperature at night, with 70% relative humidity and a 16-hour photoperiod condition with 100 µmol m^{-2} s^{-1} light intensity. The harvesting time between the wild-type and the transgenic lines was synchronized based on differences in inflorescence development and subsequent flowering time. To synchronize flowering, *JUB1OX* individuals were planted earlier, and their inflorescence stems were harvested 65 days after sowing for stem P_{50} and stem anatomical measurements. Col-0 and *jub1kd* plants were grown 10 days later, and their inflorescence stems were harvested 55 days after sowing (Supplementary Figure S1).

Tomato plants

The seeds of each genotype were sowed in Murashige and Skoog (MS) agar medium containing 1% (w/v) sucrose. After three weeks, the seedlings with sufficiently developed roots were transferred to 15x15x19 cm (=3.3 L) pots. Pots contained a mixture of soil (basis biomix, Lensli®

substrates, Bleiswijk, the Netherlands), vermiculite and sand (ratio 25:8:2), and 3 spoons of osmocote fertilizer. All pots were placed in the same growth chamber with 70% relative humidity, 24 °C temperature, with a 16-hour photoperiod condition. (Supplementary Figure S1).

Generating stem vulnerability curves (VCs)

Cavitron experiments in Arabidopsis

At the Institute of Biology Leiden, Arabidopsis plants were harvested with roots, leaves, and flowers still intact. These individuals were then immediately wrapped in wet tissue paper and placed in plastic bags to prevent dehydration during the shipment to the PHENOBOIS platform (University of Bordeaux, France) for the Cavitron centrifuge measurements, which were carried out within a week of harvest. The roots were cut at the basal part of the inflorescence stems and the stems were trimmed to a length of 27 cm to match the standard Cavitron rotor. This 27 cm length exceeds the maximum vessel length of Col-0, which is only 4 cm (Tixier *et al.*, 2013), thereby preventing the open-vessel artefact. The siliques, leaves, and flowers were removed from the segments underwater right before placing the inflorescence stems in the Cavitron rotor. The xylem vulnerability to embolism was evaluated by measuring the water flow through the inflorescence stems via the increase of cavitation induced by lowering the xylem pressure at the middle part of stems during the spinning (Cochard, 2002; Cochard *et al.*, 2005). The negative pressure was gradually increased by -0.2 to -0.4 MPa in each spinning step. The degree of embolism in the xylem segment was then quantified as the percentage loss of conductivity (PLC). The PLC was calculated as

$$PLC = 100 \text{ X } (1 - (K/K_{max}))$$

where K is the decreased hydraulic conductivity due to embolisms. K_{max} (m^2 MPa^{-1} s^{-1}) is the maximum hydraulic conductivity which was calculated when stem segments were fully functioning (no embolism) at a low spinning speed (near 0 MPa). The embolism formation at every rotation speed was measured using the Cavisoft software (Cavisoft v1.5, University of Bordeaux, France) and fitted the data points to reconstruct the VCs using a sigmoid

function based on the NLIN procedure in SAS 9.4 (SAS Institute, Cary, NC, USA) (Pammenter and Van der Willigen, 1998):

$$PLC = 100 \div [1 + exp\ (\frac{S}{25} \times (P - P_{50}))$$

where S (MPa^{-1}) is the slope of the VC at P_{50}. P is the xylem pressure used at each rotation step, and P_{50} is the xylem pressure inducing 50% loss of hydraulic conductivity. We used seven to nine individuals to generate one vulnerability curve due to the low hydraulic conductivity of Arabidopsis. Four to eight VCs were constructed for each genotype.

Optical technique measurements in tomato

The tomato plants with intact roots and leaves were transferred to the hydraulic laboratory at Naturalis Biodiversity Center (Leiden) and harvested. To prepare the plants for embolism visualization using the optical technique (Brodribb *et al.*, 2017*a*), most of the soil was carefully removed from the root system using water to speed up the drying process. The stems were then secured underneath a stereomicroscope equipped with a camera and fixed with tape to minimize any movement during drought-induced shrinkage. Next, a razor blade was used to carefully remove the stem cortex to expose the xylem to the camera. Hydrogel was applied to the exposed surface to enhance light transmission and minimize the evaporation (Brodribb *et al.*, 2017*a*). To visualize and quantify emboli in the stems through time, the plants were automatically photographed at five-minute intervals until the leaves were completely dry, and impossible to measure the water potential; this took approximately one week. Stem water potential was monitored in bagged leaves two to three times a day with a Scholander's pressure chamber (PMS Instrument Company, Albany, Oregon, USA). Fiji software (Schindelin *et al.*, 2012) and the OSOV toolbox plugin were used to analyze the optical data, following the open-source OV protocols on GitHub (www.opensourceov.org). The formation and spread of emboli over time were determined by subtracting the differences in pixels in the major veins (1st to 3rd-order veins) between subsequent images. Background noise, mainly caused by tissue shrinkage, was removed using mild filters for noise removal and manual inspection of the image and pixels. The VCs were reconstructed using the same sigmoid function (as in Arabidopsis mentioned above). Four to seven VCs were constructed for each genotype.

Stem anatomy

To study stem anatomy, three representative stems per genotype of both Arabidopsis and tomato were randomly selected for light microscopy (LM) and transmission electron microscopy (TEM) observations. In Arabidopsis, the middle part of the 27 cm inflorescence stem segments, where negative pressures were applied during Cavitron measurements, were sectioned to obtain anatomical traits data. In tomato, basal stem parts were selected from areas close to the area where embolism resistance was measured. The features measured from this part provided accurate information linking anatomical traits and embolism resistance (P_{50}). The measured traits are shown in Supplementary Table S1. We used ImageJ (National Institutes of Health, Bethesda, MD, USA) to measure the anatomical features in digital images from both LM and TEM observations, following the recommendations by Scholz *et al.* (2013).

Light microscopy

Arabidopsis

One cm long pieces of inflorescence stems were stored in 70% ethanol. The fixed samples were then gradually infiltrated and embedded in LR-White resin (Hamann *et al.*, 2011). The embedded samples were sectioned at 4 µm thickness using a rotary microtome (Leica RM 2265, Leica, Eisenmark Wetzlar, Germany) with disposable tungsten carbon blades. Then, the sections were heat-fixed onto the slides, stained with 1% (w/v) toluidine blue (VWR Chemicals BDH., Radnor, PA, USA), and mounted with DPX new-100579 mounting medium (Merck Chemicals, Amsterdam, the Netherlands). Finally, the anatomical traits were observed using a Leica DM2500 light microscope and photographed with a Leica DFC-425 digital camera (Leica microscopes, Wetzlar, Germany).

Tomato

The basal parts of the stems were cut into 40 µm thick transverse sections using a sliding microtome (Reichart) with N35 microtome blades. The sections were then bleached with household bleach containing 3% sodium hypochlorite (Acros), rinsed with demi water, and stained with a mixture of Safranin O (Chroma) and Alcian Blue (Sigma-Aldrich) in a ratio 35: 65 (Lens *et al.*, 2007). The safranin was prepared as a 1% solution in 50% ethanol. The 1% alcian blue stain was dissolved in pure water. Subsequently, the stained sections were dehydrated in a series of ethanol (50%, 70%, and 96% respectively), treated with a 1:1 combination of 96% ethanol and the histological clearing agent Limonene (HISTO-CLEAR, EMS), and afterward cleared with 100% Limonene and finally mounted on a microscope slide using Euparal green (Chroma). The sections were observed using an AXIO Imager.M2 (Zeiss) motorized microscope with a camera and photographed using Axiovision software.

Transmission electron microscope (TEM)

The 1 cm long stem pieces of Arabidopsis and tomato were fixed in Karnovsky's fixative for 48 h (Karnovsky, 1965), adjacent to the stem segments sampled for light microscopy. The samples were rinsed with 0.1 M cacodylate buffer and post-fixed with 1% buffer osmium tetroxide, and then stained with 1% uranyl acetate. The stained samples were dehydrated in a series of ethanol: 1% uranyl acetate replacement, with increasing concentration of ethanol. The dehydrated samples were then infiltrated with Epon 812n (Electron Microscopy Sciences, Hatfield, UK) and placed in the oven (60°C) for 48 h. The Epon blocks were cut into semi-thin (2 µm) and ultra-thin (90-95 nm) sections using a Leica EM UC7 ultramicrotome with a diamond knife. The sections were dried and mounted on film-coated copper slot grids, and post-stained with uranyl acetate and lead citrate. The sections were observed with a JEM-1400 Plus TEM (JEOL, Tokyo, Japan) with an 11-megapixel digital camera (Quemesa, Olympus).

Drought treatment

Arabidopsis

Seeds of each genotype were sown directly in 6x6x7 cm (=0.25 L) pots with the same ratio of soil and sand mixture (4.5:1) at different times to synchronize flowering (35 days after sowing for Col-0 and A-*jub1kd* and 45 days after sowing for A-*JUB1OX*). The weight of the pot with dry and saturated soil was controlled. The plants were grown in a growth chamber under controlled conditions similar to those used for anatomical and stem P_{50} measurements. During the experiment, thirty individuals of each genotype were equally divided into a control (well-watered) and a drought batch. The control group of plants received daily watering to keep the soil consistently hydrated, whereas the drought batch experienced a water deficit by completely abstaining from watering for three weeks, starting one week prior to flowering.

Tomato

The tomato plants used in the drought experiment were grown in the same 3.3 L pots and under the same condition as those used for the anatomical and stem P_{50} measurements. After 55 days after potting, plants of both genotypes were randomly assigned to control and drought treatments (10 control and 10 drought individuals). The control plants were well-watered every day, while plants from the drought group did not receive any water for 10 days.

Leaf water potential (Ψ_l), stomatal conductance (g_s), and CO_2 assimilation rate (A)

Arabidopsis

The leaf water potential of well-watered and drought batches was measured every day until the end of the experiment (15-17 days), starting from a 7-d water deficit which is the required time to dehydrate the moisturized soil in the pots of the drought batch. To carry out the daily measurements, three mature rosette leaves, one from the control batch and two from the drought batch, were covered with aluminum foil for 30

minutes before the measurements. The leaf discs were then cut from the wrapped leaves and placed in the PSYPRO device (Wescor, Inc., Logan, UT, USA) to measure leaf water potential. Stomatal conductance (g_s, mmol m^{-2} s^{-1}) was measured daily on the mature rosette leaves that were close to those used for water potential measurements, using an SC-1 leaf porometer (METER Group, Pullman, WA, USA). The g_s was measured using Auto Mode configuration with desiccant. Due to the small size of Arabidopsis leaves, we encountered limitations in using Targas-1 (PP systems, Amesbury, MA, USA) for measuring stomatal conductance and CO_2 assimilation rate. As a result, we were unable to obtain data on CO_2 assimilation rate in Arabidopsis.

Tomato

The Ψ_l measurements were carried out daily in both control and drought plants starting from the first day of withholding water until the end of the drought experiment (10 days). Four to five mature leaves of each genotype were bagged in aluminum zip-lock bags for at least 30 minutes before the measurements. The leaves were then cut at the base of the petiole with a fresh razor blade and Ψ_l was measured using a Model 1000 Pressure Chamber Instrument (PMS Instrument Company, Albany, Oregon, USA) (Rodriguez-Dominguez *et al.*, 2022). The g_s of the mature leaves was measured every day using an SC-1 leaf porometer (METER Group, Pullman, WA, USA) with the same mode as the one used for Arabidopsis and compared with a Targas-1 Portable Photosynthesis System (with a LED light unit; PP systems, Amesbury, MA, USA). To determine the water potential at 90% of the stomatal closure (Ψ_{gs90}), the stomatal conductance of both species was fit according to the following sigmoid function for each genotype using the NLIN procedure in SAS:

$$g_s = g_{sm} \div [1 + \exp (S \times (\Psi_{gs} - \Psi_{gs50}))]$$

where g_{sm} is the maximal stomatal conductance for $\Psi_l = 0$. S is the slope of the curve, and Ψ_{gs50} is the water potential inducing 50% stomatal closure.

Stomatal conductance data obtained from both the porometer and the Targas-1 instrument showed no significant differences between them, as shown in Supplementary Figure S2. Consequently, we chose to utilize the g_s data acquired from the Targas-1 instrument, along with the CO_2 assimilation rate data, for our subsequent analyses.

Stomatal safety margin (SSM)

The SSM was defined as the difference between the leaf water potential at 90% stomatal closure and stem P_{50} (Martin-StPaul *et al.*, 2017). It can be calculated from the fitted curve (Ψ_{gs90}) and the water potential at 50% loss of stem conductivity (P_{50}) as follows:

$$SSM = \Psi_{gs90} - P_{50}$$

Statistical analysis

The statistical analyses of all traits studied were performed using R version 3.6.3 in R Studio version 1.2.5033. A *P*-value of <0.05 was considered significant for all differences observed. Initially, general linear models were used to assess differences in embolism resistance (P_{50}, P_{12}, and P_{88}) and anatomical features among the genotypes studied, followed by a Newman-Keuls post-hoc test. Multiple linear regression was then applied to determine the anatomical traits (predictive variables) that explain differences in embolism resistance (responsive variables, including P_{50}, P_{12}, and P_{88}). Collinearity between variables was checked to select predictors, and the 'step' function (stats package; R Core Team, 2016) was used to obtain the most parsimonious linear regression model based on the least Akaike information criterion (AIC). Residuals, heteroscedasticity, skewness and kurtosis, and variance inflation factor (VIF) were checked once the best model was obtained. The relative importance of each explanatory variable was analyzed to determine the variable that best explains P_{50}. Pearson's correlation was used to plot the relationship between P_{50} and predictive variables. Lastly, a generalized linear mixed model was used to investigate whether the different genotypes exhibited different g_s in well-watered control conditions. The genotypes were used as a fixed effect using the GLIMMIX procedure in SAS (SAS 9.4; SAS Institute).

Results

Phenotypic variation in drought responses in Arabidopsis and tomato

After subjecting Arabidopsis and tomato plants to a water deficit treatment for a period of up to 17 days and 10 days, respectively, we observed notable differences in the phenotypes of the drought-treated batches compared to the well-watered plants. The drought-treated plants were consistently smaller in size than the well-watered plants for each species, and the leaves of the drought-treated A-T-wild-types and A-*jub1kd* individuals showed strong signs of leaf wilting, as well as a higher incidence of yellow leaves and leaf senescence (Figure 1). Interestingly, the *JUB1OX* transgenic lines of both species demonstrated no leaf wilting, and the leaves retained their green color without any observation of leaf senescence (A-*JUB1OX* and T-*JUB1OX* shown in Figure 1).

Leaf water potential (Ψ_l), dynamics of stomatal conductance (g_s), and CO_2 assimilation rate (A) under drought stress

In well-watered plants, Ψ_l was similar for each species, with Arabidopsis displaying a value of -0.5 MPa, and tomato exhibiting a range between -0.2 to -0.25 MPa for all genotypes studied (Figure 2A, 2C; Supplementary Figure S3). During the onset of drought, we observed a consistent difference between Ψ_l decline in *JUB1OX* genotypes and the other genotypes studied: A-T-*JUB1OX* plants maintained a stable and high Ψ_l for several days before exhibiting a gradual decline, while A-T-wild-types, and A-*jub1kd* mutant exhibited an earlier and more rapid Ψ_l decline (Figure 2A, 2C). This more rapid Ψ_l decline in the latter three genotypes means that P_{50} was reached after only 9 days of drought (T-wild-type) and 11 days of drought (A-wild-type and A-*jub1kd*); T- and A-*JUB1OX* plants reached P_{50} much later: later than 10 days after onset of water deficit and at day 14, respectively (Figure 2A, 2C; Table 1).

Figure 1 Representative images showing phenotypic variation between well-watered and drought-treated individuals of Arabidopsis (68-72 days after sowing) and tomato (65 days after potting) across all the genotypes studied, taken at the end of the drought treatment (up to 17 days of water deficit in Arabidopsis, and 10 days of water deficit in tomato). At least seven plants per genotype and conditions were analyzed.

The patterns of stomatal conductance (g_s) showed more variation between the two species. In Arabidopsis, the stomatal conductance of A-wild-type and A-*jub1kd* was similarly high before drought, approximately 360 $mmolm^{-2}s^{-1}$, and gradually declined during the first week of drought. This was followed by a steep decline in g_s on day 7 and day 9, respectively, until they reached 90% of stomatal closure (g_{s90}) after 10-11 days of water deficit. A-*JUB1OX* genotype exhibited lower g_s at well-watered conditions (255 $mmolm^{-2}s^{-1}$) and maintained a gradual decline over time until it reached g_{s90} a few days later than the other two genotypes (14 days after onset of drought) (Figure 2B; Table 1). The well-watered tomato plants showed another pattern. The T-*JUB1OX* transgenic line displayed an equally high g_s as the T-wild-type, with a value of 420 $mmolm^{-2}s^{-1}$. Quickly after the onset of drought, g_s of T-wild-type declined steadily until it reached g_{s90} on day 6 of drought, while T-*JUB1OX* exhibited first a g_s plateau between day 3-6 after the onset of water deficit before declining rapidly, reaching g_{s90} one to two days later than the wild-type (Figure 2D; Table 1; Supplementary Figure S3).

Under well-watered conditions, the T-*JUB1OX* genotype displayed a significantly higher CO_2 assimilation rate (A) compared to the T-wild-type ($F = 9.97$, $P = 0.002$). Furthermore, the *JUB1OX* genotype could maintain a greater CO_2 assimilation rate and exhibited a slower decline in assimilation than the wild-type during the drought experiment (Figure 2E; Supplementary Figure S3C).

Stem vulnerability to embolism based on vulnerability curves (VCs)

We observed different patterns of stem vulnerability between Arabidopsis and tomato among the genotypes studied. In Arabidopsis, the wild-type demonstrated the highest resistance to embolism, with a P_{50} value of -2.14 MPa, followed by A-*JUB1OX* (P_{50}: -1.58 MPa) and A-*jub1kd* (P_{50}: -1.37 MPa). The slope of the VCs was more gradual in A-Col-0, but steeper in A-*JUB1OX* and A-*jub1kd* (Figure 3A). In tomato, however, T-wild-type and T-*JUB1OX* exhibited no significant difference in embolism resistance and slope, with P_{50} values of -1.54 and -1.45 MPa, respectively (Figure 3B). The P_{12} values (stem water potential at the onset of embolism) showed the same pattern in both Arabidopsis and tomato, with wild-types having less negative P_{12} values than the overexpression transgenic lines (Table 1). The P_{12} values of each genotype were significantly different from each other ($F = 2.317$; P

< $2e^{-16}$). In contrast, the P_{88} values showed the opposite pattern, with wild-types of both species exhibiting more negative values than *JUB1OX* genotypes. The P_{88} values of each genotype in both species were also significantly different from each other (F = 2.704; $P < 2e^{-16}$) (Table 1).

Table 1 The hydraulic data of Arabidopsis and tomato genotypes studied

Genotypes	P_{12} (MPa)	P_{50} (MPa)	P_{88} (MPa)	Ψ_{gs90} (MPa)	SSM (MPa)	Days until 90% stomatal closure	Days until P_{50}
A-Col-0	-0.78	-2.14	-3.51	-0.9	1.24	10	11
A-*JUB1OX*	-0.94	-1.58	-2.21	-1.03	0.55	14	14
A-*jub1kd*	-0.96	-1.37	-1.78	-1.05	1.32	11	11
T-MM	-1.12	-1.54	-1.96	-0.55	0.99	6	9
T-*JUB1OX*	-1.21	-1.45	-1.69	-0.43	1.02	7	does not reach P_{50}

P_{12} = stem water potential at 12% loss of hydraulic conductivity, P_{50} = stem water potential at 50% loss of hydraulic conductivity, P_{88} = stem water potential at 88% loss of hydraulic conductivity, Ψ_{gs90} = leaf water potential at 90% stomatal closure, SSM= stomatal safety margin

Stomatal safety margin (SSM)

All the genotypes studied in both Arabidopsis and tomato exhibited positive SSMs. In Arabidopsis, the widest SSM was observed in A-wild-type with a value of 1.24. The A-*JUB1OX* and A-*jub1kd* mutants had narrower SSM values of 0.55 and 0.32, respectively. In tomato, T-*JUB1OX* showed a similar SSM compared to T-wild-type with values of 1.02 and 0.99, respectively (Table 1).

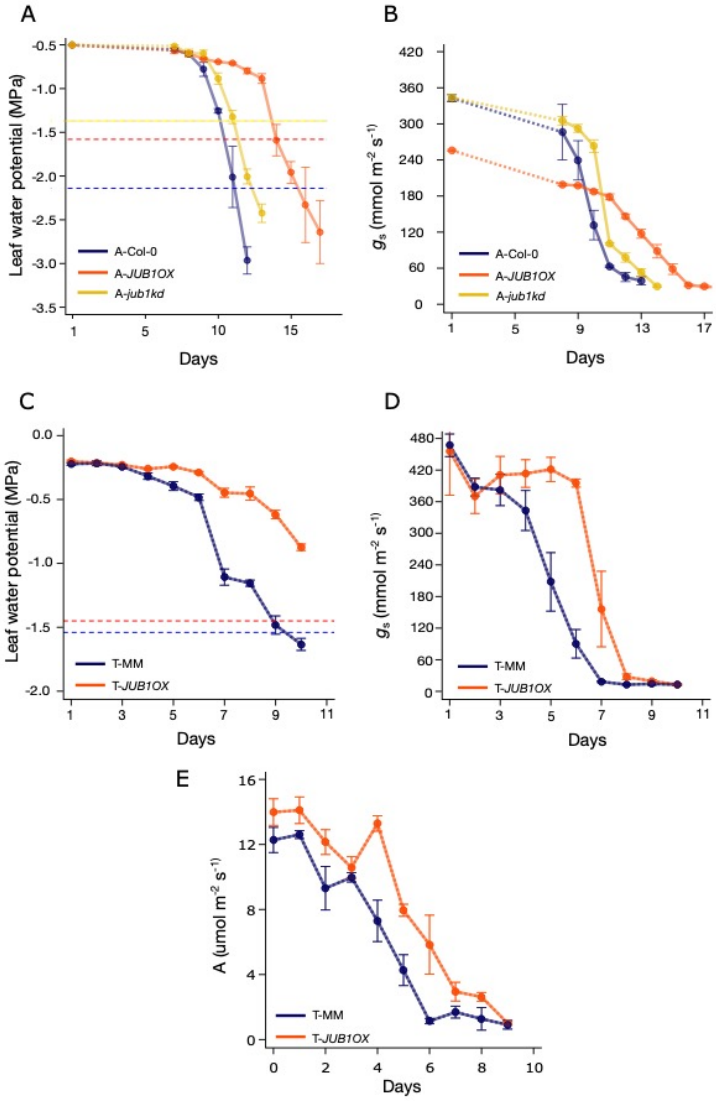

Figure 2 Drought-responsive traits for the Arabidopsis and tomato genotypes measured during the drought experiment. (A) The leaf water potential (Ψ_l) over time. (B) The stomatal conductance (g_s) of Arabidopsis over time. (C) Tomato Ψ_l over time. (D) Tomato g_s over time. (E) Tomato CO_2 assimilation (A) over time. Colours refer to the genotype studied: wild-type (blue); *JUB1* overexpression (orange); *JUB1* knocked down (yellow).

Differences in stem anatomical traits among genotypes studied

Our study revealed significant differences in various anatomical traits among genotypes within both species. Interestingly, in both Arabidopsis and tomato, the wild-types had thicker intervessel pit membranes (T_{PM}) (Supplementary Figure S4) (F = 237.4, P = 1.94e^{-06} and F = 10.76, P = 0.03, respectively) and a higher proportion of fiber wall area per fiber cell area (PF_WF_A) (F = 54.53, P = 0.0001 and F = 334.8, P = 5.25e^{-05}, respectively) compared to the overexpression transgenic lines (*JUB1OX*), while the knockdown line in Arabidopsis (A-*jub1kd*) had the thinnest T_{PM} and PF_WF_A. The wild-types of both species had the widest maximum vessel diameter (D_{MAX}) compared to other genotypes, followed by *JUB1OX* transgenic lines and the *jub1kd* line in Arabidopsis (F = 12.24, P = 0.0076 and F = 46.57, P = 0.0024, respectively). Furthermore, vessel wall thickness (T_V) was significantly different among Arabidopsis genotypes, with A-Col-0 (wild-type) having the thickest vessel walls and A-*jub1kd* possessing the thinnest walls (F = 45.95, P = 0.0002), but no differences were found in tomato. Likewise, the proportion of lignified area per total stem area (P_{LIG}) showed significant differences among Arabidopsis genotypes, with A-Col-0 having the highest P_{LIG} followed by A-*JUB1OX* and A-*jub1kd* (F = 41.8, P = 3e^{-04}), whereas tomato genotypes did not show any difference. With respect to vessel grouping (V_G), we measured the highest mean value in A-*JUB1OX*, and the lowest V_G in A-Col-0 (F = 59.38, P = 0.0001), but no differences were detected in tomato. For vessel density (V_D), we found the opposite pattern: V_D of T-*JUB1OX* was significantly higher than that of the T-MM wild-type (F = 13.43, P = 0.0215), but no differences were observed among Arabidopsis genotypes.

Stem anatomical traits explaining the variation in embolism resistance

Based on the most parsimonious model obtained through multiple linear regression (AIC = -245.59), we found that the stem anatomical predictors of embolism resistance variation were T_{PM}, PF_WF_A, D_{MAX}, and T_V (R^2 = 0.910, P < 2.2e^{-16}). Among these, T_{PM} had the highest relative importance (34%) explaining P_{50} variation, followed by PF_WF_A (28%), D_{MAX} (18%), and T_V (12%) (Supplementary Figure S5A). These anatomical traits also accounted for a significant proportion of the variation in P_{12} (62 % relative importance), with T_{PM} being also the most important predictor,

responsible for almost half of the variation (R^2 = 0.6931, P = 3.699e^{-16}) (Supplementary Figure S5B). Among the predictors of P_{88} variation, PF_WF_A was found to be the most significant one with a relative importance of 41% (R^2 = 0.5269, P = 3.62e^{-11}) (Supplementary Figure S5C).

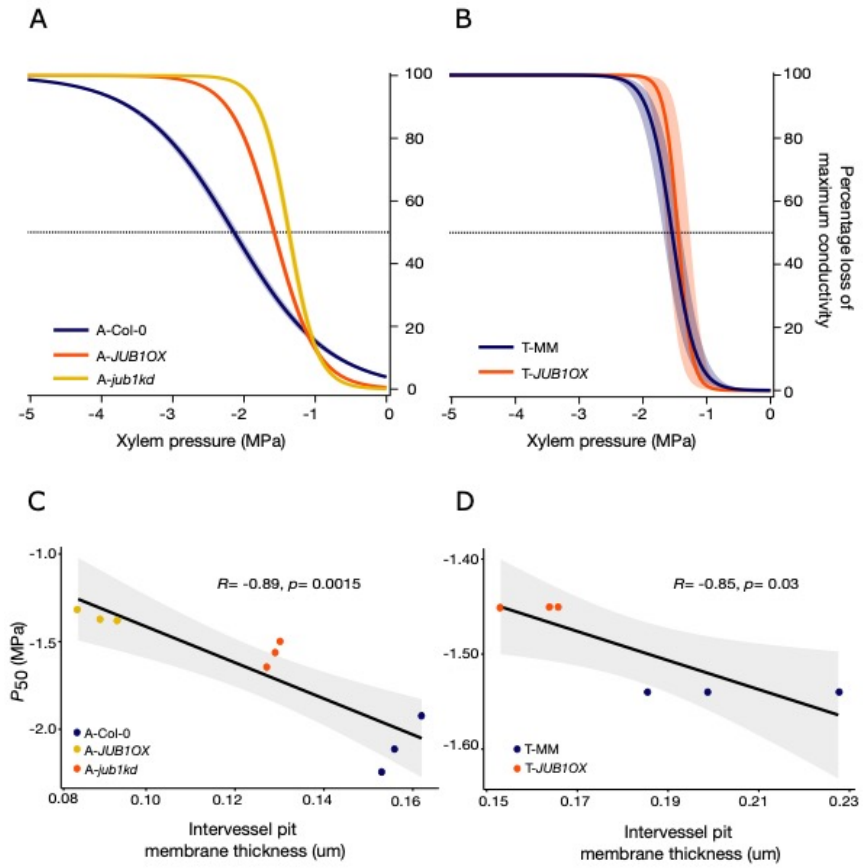

Figure 3 Mean vulnerability curves (VCs) presenting the percentage loss of conductivity (PLC) as a function of xylem pressure (MPa) of (A) Arabidopsis and (B) tomato across the genotypes studied. Shaded bands represent standard errors based on four to eight VCs per genotype. (C) The scatter plots based on Pearson's correlation analysis show the correlations of P_{50} and intervessel pit membrane thickness (T_{PM}) of Arabidopsis and (D) tomato. Colours refer to the genotype studied: wild-type (blue); *JUB1* overexpression (orange); *JUB1* knocked down (yellow).

Discussion

This study presents for the first time a set of anatomical and hydraulic traits of stems and leaves in Arabidopsis and tomato plants to elucidate the *JUB1*-mediated mechanisms underlying the increased drought tolerance observed. Interestingly, among all the traits observed during the drought treatment, only the high and stable leaf water potential is in agreement with the increased drought resilience behaviour of *JUB1* overexpression (*OX*) plants compared to the wild-type plants in both species. Interestingly, the underlying anatomical and physiological modifications triggered by *JUB1* overexpression are not in line with traits associated with drought resilience as observed in many other studies, opening new perspectives on the role of *JUB1* in plant response to drought.

High leaf water potential (Ψ_l) is central in JUB1OX plants' drought resilience

The improved drought tolerance of the *JUB1OX* plants in both Arabidopsis and tomato compared to the wild-types and the *JUB1* knockdown line in Arabidopsis (A-*jub1kd*) is attributed to their capacity to maintain high leaf water potential (Ψ_l) during drought stress (Figures 1-2). In Arabidopsis, a lower initial stomatal conductance (g_s) in A-*JUB1OX* compared to wild-type, gradually decreasing up to 10 days of withholding water followed by a steeper decline, is consistent with a high and relatively stable Ψ_l up to 13 days of water deficit (Figure 2A, 2B). In contrast, the Arabidopsis wild-type and A-*jub1kd* showed a considerably higher g_s followed by a more rapid decline of stomatal conductance after 8-9 days and a subsequent steep drop of Ψ_l at 9-10 days during drought (Li *et al.*, 2017; Dayer *et al.*, 2020; Lemaire *et al.*, 2021*a*; Welsch, 2022). Interestingly, A-*JUB1OX* reached full stomatal closure later than the wild-type and A-*jub1kd* (Figure 2B), enabling extended photosynthetic activity without risking detrimental levels of drought-induced embolism (Thonglim *et al.*, 2023). In contrast, *JUB1OX* in tomato displayed an equally high initial g_s compared to wild-type tomato plants and kept its stomata fully open for six days before showing a dramatic g_s drop (Figure 2D). Despite the greater loss of water through transpiration, T-*JUB1OX* plants were able to maintain a high Ψ_l for two more days (up to eight days of water deficit) before a more drastic decline compared to the T-MM wild-type (Figure 2C). In other words, the inconsistency in g_s differences between the overexpression genotypes and

the wild-types in Arabidopsis and tomato suggest that stomatal conductance does not explain why leaf water potential in *JUB1OX* plants remains high for a longer period of drought stress.

Plants can exhibit markedly different mechanisms to drought within a single species

Contrary to what we expected, the remaining hydraulic and stem anatomical traits that have often been shown to be associated with increased drought resilience in Arabidopsis and other species, such as more negative stem P_{50}, broader stomatal safety margins, thicker intervessel pit membranes and higher levels of stem lignification (Thonglim *et al.*, 2021, 2023; Lens *et al.*, 2022) are not observed in the more resilient *JUB1* overexpression lines in both Arabidopsis and tomato plants. Especially the presence of thinner intervessel pit membranes and less lignified stems in both A-*JUB1OX* and T-*JUB1OX* plants compared to wild-type plants is remarkable given the relevance of these traits in the improved drought response of Arabidopsis and beyond (Li *et al.*, 2016; Dória *et al.*, 2018; Thonglim *et al.*, 2021, 2023; Guan *et al.*, 2022; Lens *et al.*, 2022). It is remarkable to see that even in species with a short life cycle, such as Arabidopsis, substantially different strategies can be employed to acquire a certain level of drought tolerance. Therefore, our observations demonstrate that the increased drought tolerance of *JUB1* overexpression plants is not due to their drought-responsive anatomical and hydraulic traits. Instead, the only consistent observed trait that is in line with the improved drought stress behaviour of the A-T-*JUB1OX* plants is their ability to maintain high leaf water potential for a longer period of water shortage.

Suggested mechanisms leading to increased drought response of JUB1OX plants

Our results clearly indicate that the improved drought tolerance of *JUB1* overexpression plants is not due to their anatomical and hydraulic traits that are otherwise known to play a role in drought-induced mechanisms. But what are the potential drought-related traits that we have missed in our study? From the literature, there are two *JUB1*-mediated candidates that could offer an explanation for the elevated Ψ_l during the period of water deficit. One line of research indicates that *JUB1*

overexpression leads to increased levels of the amino acid proline (Pro) in various species (Wu *et al.*, 2012; Shahnejat-Bushehri *et al.*, 2017; Tak *et al.*, 2017; Alshareef *et al.*, 2019; Welsch, 2022). Proline accumulation is crucial for the plants' ability to overcome lower water potential, as it acts as an osmolyte, facilitating additional water uptake and buffering the immediate impact of water scarcity. Furthermore, proline helps with cellular osmotic adjustment and stabilizes sub-cellular structures, thereby contributing to enhanced drought tolerance in plants (Heuer, 2010; Blum, 2017; Hasanuzzaman *et al.*, 2019; Ahmad *et al.*, 2020; Ozturk *et al.*, 2021). Additionally, the overexpression of *JUB1* could also result in a reduction of reactive oxygen species (ROS), particularly H_2O_2, through the accumulation of DELLA proteins (Shahnejat-Bushehri *et al.*, 2012, 2016; Wu *et al.*, 2012; Ebrahimian-Motlagh *et al.*, 2017; Thirumalaikumar *et al.*, 2018). ROS accumulation during stress can cause oxidative damage to various cellular components, leading to reduced photosynthetic efficiency, reduced cell membrane stability, metabolic dysfunction, and ultimately cell death (Benjamin and Nielsen, 2006; Cruz De Carvalho, 2008; Hanin *et al.*, 2011; Choudhury *et al.*, 2013, 2017). Unfortunately, our study did not analyze the concentration of osmoprotectants nor ROS, as this will be the focus of a follow-up study that will further disentangle whether and how *JUB1* regulates osmoprotectants accumulation and ROS mitigation at the molecular level. We did, however, observe that T-*JUB1OX* maintained higher CO_2 assimilation rates under well-watered conditions (Supplementary Figure S3C), and exhibited a slower decline of CO_2 assimilation rates during drought (compared to T-wild-type; Figure 2E) implying more efficient photosynthesis and possibly a faster production of osmoprotectants and antioxidant compounds under both drought and well-watered conditions. The potential role of *JUB1* serves as a promising initial step to dive deeper into the *JUB1*-mediated mechanistic role of improved drought tolerance, and further experiments should be conducted to confirm this.

In conclusion, the key factor for enhancing drought response in *JUB1OX* plants is the preservation of a high leaf water potential. However, unlike other Arabidopsis genotypes, none of the studied stem anatomical features or hydraulic traits, which were previously linked to enhanced drought tolerance, are involved in the underlying mechanisms. This suggests that *JUB1* acts on different gene regulatory pathways leading to drought resilience, possibly via increased osmoprotectants and/or decreased ROS,

compared to those activated in other resilient Arabidopsis genotypes which tend to develop more embolism resistant stems that are more lignified and have thicker intervessel pit membranes. The presence of multiple, contrasting drought strategies in a single annual species is remarkable and highlights the adaptive abilities of plants to cope with drought stress. It is therefore imperative to perform drought experiments across multiple accessions/genotypes in, for instance, crops to gain a better picture of their full potential to respond to drought.

Acknowledgements

We would like to thank Rob Langelaan (Naturalis Biodiversity Center) and Gaëllle Capdeville (BIOGECO INRA) for technical support in TEM observations and Cavitron centrifuge measurements, respectively. This work was funded by a PhD scholarship awarded by the Institute for the Promotion of Teaching Science and Technology (IPST), Thailand, and by the Dutch Research Council NWO (grant ALWOP.488).

Supplementary data

Supplementary Table S1 The anatomical characters and hydraulic values measured with acronyms, definitions, calculations, units, and microscope techniques

Acronyms	Definition	Calculation	Number of measurements	Unit	Technique
A	CO_2 assimilation	$A = - [((C_{out} - C_{in}) \times W) + (C_{out} \times E)]$	At least 1 control sample and 2 drought samples for each measurement	µmol $m^{-2}s^{-1}$	Targas-1
A_F	Fiber cell area	Area of single xylem fiber in cross-section	Min. 30 fibers	$µm^2$	LM
A_{FL}	Fiber lumen area	Area of single xylem fiber lumen in cross-section	Min. 30 fibers	$µm^2$	LM
A_{FW}	Fiber wall area	$A_F - A_{FL}$ for the same fiber	Min. 30 fibers	$µm^2$	LM
A_{LIG}	Lignified stem area	Total xylem area + fiber caps area + lignified pith cell area in cross-section	9 stems per accession	mm^2	LM
A_S	Total stem area	Total stem area in cross-section	9 stems per accession	mm^2	LM
Day_{90}	Days until reaching 90% of stomatal closure	-	-	days	-
D	Diameter of vessels	$D = (\sqrt{4A}/\pi)$	Min. 50 vessels	µm	LM
D_{MAX}	Maximum vessel lumen diameter	Diameter of single vessel	Min. 30 vessels	µm	LM
D_{PC}	Pit chamber depth	Distance from the relaxed pit membrane to the inner pit aperture	Min. 25 pits	µm	TEM
g_s	Stomatal conductance	-	1 control sample and 2 drought samples each measurement	mmol $m^{-2}s^{-1}$	Porometer
SSM	Stomatal safety margin	$\Psi gs_{90} - P_{50}$	1 SSM per accession	MPa	-

Acronyms	Definition	Calculation	Number of measurements	Unit	Technique
P_{50}	Stem water potential at 50% loss of hydraulic conductivity	-	8 values per each accession	MPa	Cavitron centrifuge
P_{88}	Stem water potential at 88% loss of hydraulic conductivity	-	8 values per each accession	MPa	Cavitron centrifuge
$P_{FW}F_A$	Proportion of fiber wall area per fiber cell area	A_{FW}/A_F for the same fiber; a measure of xylem fiber wall thickness	Min. 30 fibers	-	LM
P_{LIG}	Proportion of lignified area per total stem area	A_{LIG}/A_S	9 stems per accession	-	LM
T_{PM}	Intervessel pit membrane thickness	Thickness of intervessel pit membrane measured at its thickest point	Min. 25 pit membranes	µm	TEM
T_V	Vessel wall thickness	Thickness of a single vessel wall	Min. 30 vessels	µm	LM
$(T_{VW}/D_{MAX})^2$	Theoretical vessel implosion resistance	$(T_{VW}/D_{MAX})^2$	Min. 30 measurements	-	LM
V_D	Vessel density	Number of vessels per mm^2	Min. 5 measurements	No. of vessel per mm^2	LM
V_G	Vessel grouping index	Ratio of total number of vessels to total number of vessel groupings (incl. solitary and grouped vessels)	Min. 50 vessel groups	-	LM
Ψ_{gs90}	Leaf water potential at 90% loss of stomatal conductance	-	At least 3 control and 3 drought samples each measurement	MPa	PSYPRO Meter and Pressure chamber
Ψ_l	Leaf water potential	-	At least 3 control and 3 drought samples each measurement	MPa	PSYPRO Meter and Pressure chamber

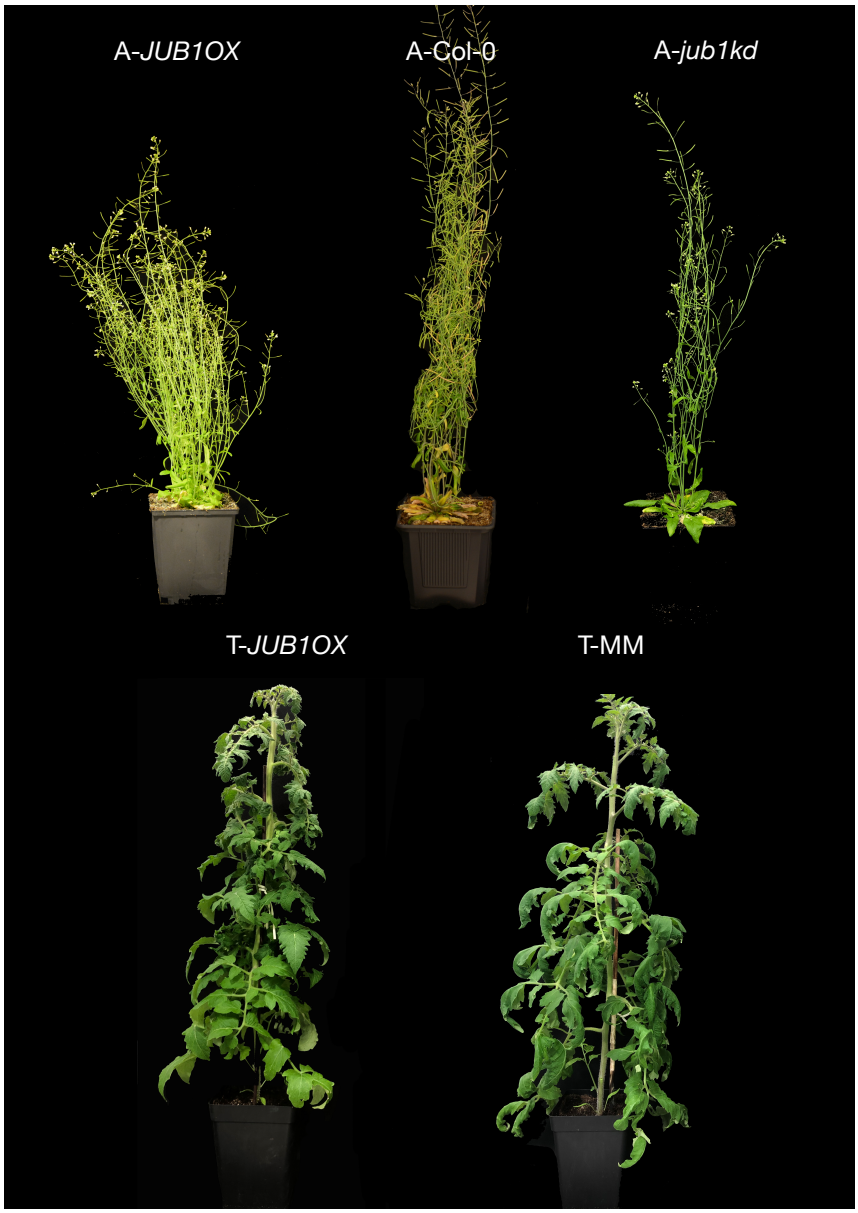

Supplementary Figure S1 Growth form of genotypes of Arabidopsis and tomato used for stem anatomical and stem P_{50} studies. A-*JUB1OX* (top left, 65d after sowing), A-Col-0 (top middle, 55d after sowing), A-*jub1kd* (top right, 55d after sowing), T-*JUB1OX* (bottom left, 55d after potting) and T-MM (bottom right, 55d after potting).

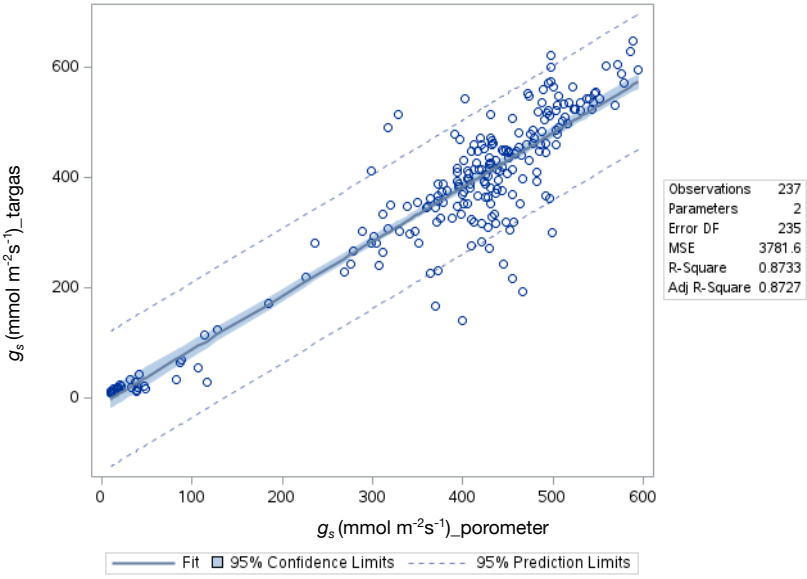

Supplementary Figure S2 The relationship between stomatal conductance (g_s) measured with Targas-1 and porometer. Shaded band represents the 95% confidence limits. The dotted lines represent 95% prediction limits.

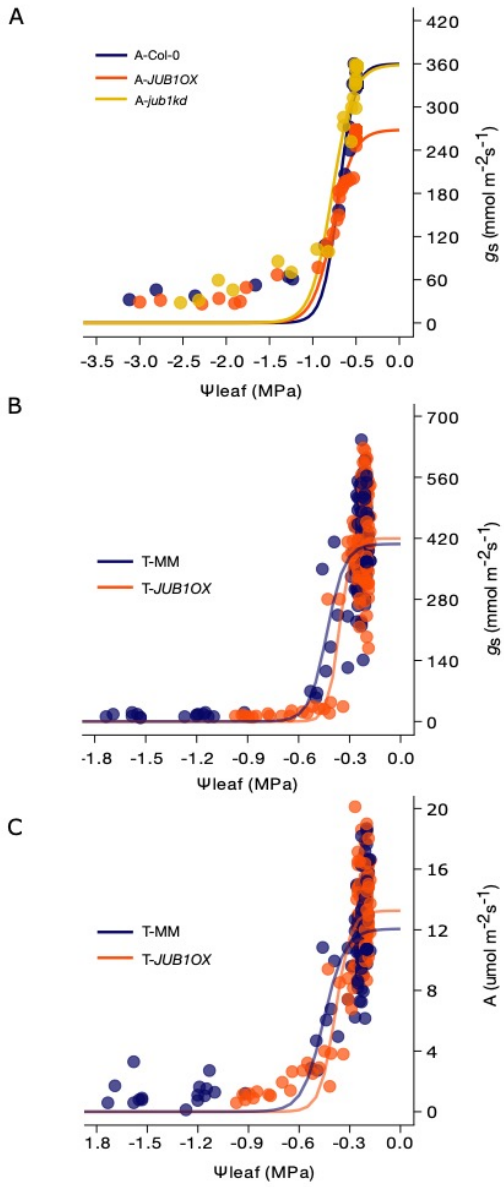

Supplementary Figure S3 The relationship between leaf water potential and stomatal conductance during the drought experiment in (A) Arabidopsis and (B) tomato. (C) The relationship between leaf water potential and CO_2 assimilation (A) of tomato. Colours refer to the genotype studied: wild-type (blue); *JUB1* overexpression (orange); *JUB1* knocked down (yellow).

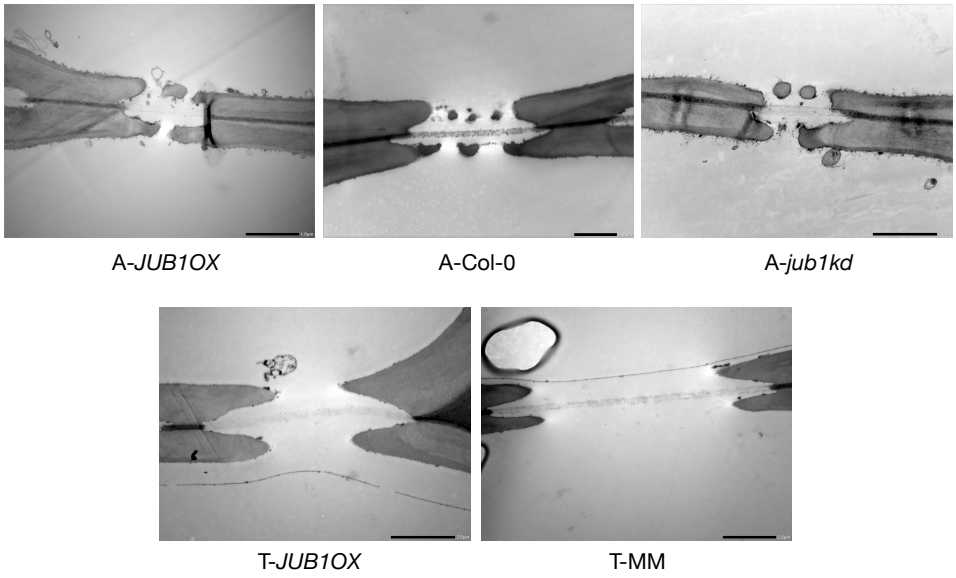

Supplementary Figure S4 TEM images of intervessel pit membranes. Scale bars = 1 μm and 2 μm.

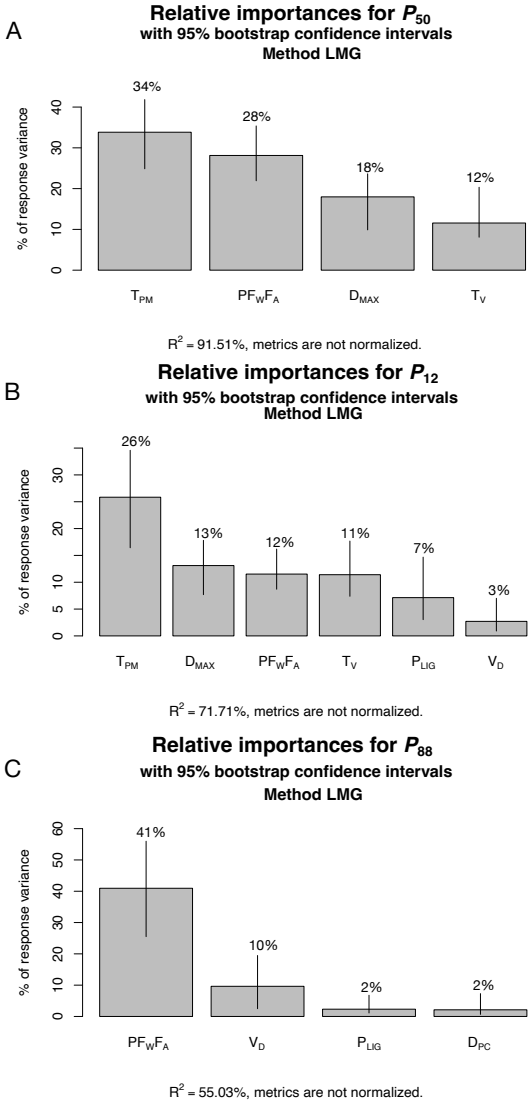

Supplementary Figure S5 The relative importance of P_{50}, P_{12} and P_{88} evaluated based on R^2 contribution averaged over orderings among regressors (Lindemann, Merenda, and Gold (LMG) method). (A) The relative importance of P_{50} variation is mainly explained by intervessel pit membrane thickness (T_{PM}) and proportion of fibre wall area per fibre cell area (PF_WF_A). (B) T_{PM} is the most important parameter explaining the relative importance of P_{12} variation. (C) The relative importance of P_{88} variation is mainly explained by PF_WF_A